

# Controlling surface dust in a tokamak

C.V. Parker<sup>a</sup>, C.H. Skinner<sup>b,\*</sup>, A.L. Roquemore<sup>b</sup>

<sup>a</sup> *Harvey Mudd College, Claremont, CA 91711, USA*

<sup>b</sup> *Princeton Plasma Physics Laboratory, P.O. Box 451, Princeton, NJ 08543, USA*

---

## Abstract

Methods to measure the inventory of dust particles and to remove dust if it approaches safety limits will be required in next-step tokamaks. A novel electrostatic dust detector, based on a fine grid of interlocking circuit traces, biased to 30 or 50 V, has been developed for the detection of dust on remote surfaces in air and vacuum environments. Impinging dust particles are detected when they create a short circuit between the traces, however this short circuit is temporary suggesting the device may be useful for the removal of dust from specific areas. The fate of the dust particles has been tracked by measurements of mass gain/loss. Heating by the current pulse caused up to 90% of the particles to be ejected from the grid or vaporized, the removal efficiency depending on the experimental geometry. We also report the first attempt at real-time dust detection in NSTX.

© 2007 Elsevier B.V. All rights reserved.

*PACS:* 52.40.Hf; 52.90.+z

*Keywords:* Dust; Erosion; Deposition; ITER; NSTX

---

## 1. Introduction

The management of dust particles is one of the serious plasma material interaction issues that needs to be resolved before ITER can study burning plasmas [1–4]. Dust in tokamaks can be produced by the disassembly of plasma facing tile surfaces or of plasma-grown co-deposited layers under the impact of ELMs or disruptions, or by the chemical agglomeration of sputtered  $C_n$  clusters [5–7]. In next-step devices the increase in duty cycle and erosion levels will cause a large scale-up in the amount of dust

particles produced. This has important safety consequences as the dust particles may be radioactive from tritium or activated metals, toxic and/or chemically reactive with steam or air. A guideline to limit the mobilisable tungsten dust to 100 kg inside the ITER vacuum vessel has been established due to its radiological hazard. To limit the hydrogen potentially generated by chemical reactions following in-vessel coolant spills or air ingress the quantity of chemically reactive dust on hot plasma facing components of the divertor is limited to less than 6 kg each of beryllium, carbon and tungsten [8]. However measuring the dust particle inventory is a challenge in existing tokamaks let alone one with the radiological environment and scale of ITER. Diagnostics that could provide assurance that ITER

---

\* Corresponding author. Tel.: +1 609 243 2214; fax: +1 609 243 2665.

*E-mail address:* [cskinner@pppl.gov](mailto:cskinner@pppl.gov) (C.H. Skinner).

is in compliance with its dust inventory limits are in their infancy. A separate challenge is demonstrating techniques that could remove dust from the tokamak, once the limits are approached.

A novel device to detect the settling of dust particles on a remote surface has recently been developed in the laboratory [9,10]. A grid of two closely interlocking conductive traces on a circuit board was biased to 30–50 V. Test particles, scraped from a carbon fiber composite tile, were delivered to the grid by a stream of nitrogen. Miniature sparks appeared when the particles landed on the energized grid and created a transient short circuit. Typically the particles vaporized in a few seconds restoring the previous voltage standoff. The transient current flowing through the short circuit created a voltage pulse that was recorded by standard nuclear counting electronics and the total number of counts was related to the mass of dust impinging on the grid. The device worked well in both atmosphere and vacuum environments. The sensitivity has been enhanced by more than an order of magnitude by the use of ultrafine grids [11]. The response to particles of different size categories was compared and the sensitivity, expressed in counts/areal density ( $\text{mg}/\text{cm}^2$ ) of particles, was maximal for the finest particles. This is a favorable property for tokamak dust which is predominantly of micron scale [1]. Larger particles produce a longer current pulse, providing qualitative information on the particle size.

In the present work we investigate the fate of carbon dust particles after they land on an energized grid and create a short circuit. Typically open circuit conditions are rapidly restored in both air and vacuum environments, indicating that the dust particles have been removed from the circuit board. We characterize the removal efficiency by measurements of the mass of the dust incident on an energized circuit board, the mass that remains on the board and the mass that appears in other locations.

## 2. Experimental setup

Simulated dust particles were obtained by scraping a carbon fiber composite tile as in Refs. [9,11]. The particles had a count median diameter of 2.9  $\mu\text{m}$ , similar to the 2.1  $\mu\text{m}$  count median diameter of dust collected in NSTX at a lower viewport at Bay B. The dust was prefiltered through a vibrating wire mesh with 104  $\mu\text{m}$  by 104  $\mu\text{m}$  square holes. About 30 mg of dust was loaded into a 2.5 cm diameter cylindrical container made from the same mesh

that was attached to a shaft on a vacuum feedthrough. In the absence of any disturbance the dust remained in the container. The dust container and circuit grid were placed inside a vacuum chamber that was evacuated to 50–100 mTorr. When desired, dust was released by applying a vibrating engraving tool to the shaft on the external side of the vacuum feedthrough. About 10 mg of particles was released in 30 s and fell evenly in a 2 cm diameter area with no clumping. This method delivered an order of magnitude more dust than the previous method [9], so that tracking dust with the available balance of readout precision of 0.1 mg was possible.

The dust removal efficiency was measured by measuring the mass of dust lost by the container and mass gained by the circuit grid and other components. The circuit board is  $22 \times 27$  mm in area of which the central  $12.5 \times 12.5$  mm grid is energized. Two systems were used to mask the unenergized area of the board (Fig. 1). The first system was a square aluminum funnel (section of a four-sided pyramid) glued to a circuit board with a 1 cm square hole in the center. This was mounted so that the hole was directly above the circuit grid. Dust destined to miss the circuit grid either slid down the funnel onto the grid, or stuck to the surface of the funnel. Dust that was ejected by the energized circuit grid could be deposited on the funnel. The second system was a ‘chimney and roof’ made of

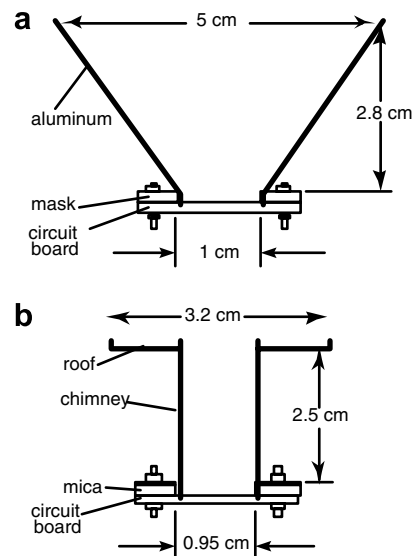


Fig. 1. Two systems used to mask the unenergized area of the circuit grid (a) a four-sided aluminum funnel and (b) a stainless steel ‘chimney and roof’.

stainless steel foil. The ‘chimney’ was a square vertical shaft 2.55 cm tall, with 0.95 cm sides. The ‘roof’ at the top of the chimney was 3.2 cm square with a 0.95 cm square hole aligned with the chimney, with raised inner and outer edges raised to contain dust. The base of the chimney was insulated from the circuit grid by a mica mask with a 0.95 cm square hole. The chimney was intended to return ejected dust to the circuit board and increase the opportunity for it to be vaporized.

In the experiment the mass of the container loaded with dust, and the mass of the circuit grid and mask components were measured individually and the items installed in the vacuum chamber. After pumpout, the vibrating tool was applied to deliver some dust to the circuit grid. Afterward the chamber was vented and the components were carefully reweighed. The dust container was weighed and transported in an aluminum foil pouch to ensure that any particles lost in transport were accounted for. Initial tests were done on an unenergized circuit grid in vacuum to compare the mass lost by the dust container to the mass gained by the circuit grid and mask (funnel, or chimney, roof and mica). These tests were repeated at least 3 times for the same conditions. It was found that the mass gained by the unenergized circuit grid and mask was 0.4–0.8 mg less than the mass loss of the dust container after 30 s of vibration. Without vibration, the circuit grid and mask did not gain mass, but the dust container still showed a decrease in mass of 0.8 mg. Glass slides placed near the circuit grid showed evidence of dust that had missed the mask, suggesting that air currents during evacuation and repressurization had caused some dust loss. Mass loss due to outgassing of water absorbed in the dust may also contribute.

The circuit board used for trials with the funnel had 50  $\mu\text{m}$  wide traces with 50  $\mu\text{m}$  spacing between traces. For the chimney configuration a 50  $\mu\text{m}$  trace/space grid was used in one vacuum measurement and for the other vacuum and air measurements 75  $\mu\text{m}$  trace/space grids were used. Both configurations were biased at 50 V with a power supply that was current limited to 60 mA. More details are in Refs. [9,11]. One of the difficulties was that the  $\sim 10$  mg of dust needed for accurate mass measurements by the available balance sometimes overloaded the circuit grid causing the bias voltage to decrease, and sometimes the resulting heat damaged the circuit traces. This was partially mitigated by reducing the vibration amplitude

which lowered the rate of dust release. Measurements in which the bias voltage permanently decreased were discarded.

### 3. Removal efficiency

The efficacy of the energized grid in removing dust is illustrated in Fig. 2. Here, one of the traces is open circuit and the incident dust accumulates in a row along the trace. On either side the traces show a greatly reduced density of dust particles.

A histogram of the average mass gained by the grid and funnel and the difference between the initial and final total mass (the ‘missing mass’) for energized and unenergized conditions is shown in Fig. 3(a). It can be seen that the energized grid ejected 91% of the dust incident on it. At the same time the fraction of dust landing on the funnel increases, as does the amount of ‘missing mass’. The dust incident on the energized grid is estimated from the mass lost by the dust container less that landing on the funnel and lost to pumpout, both for the unenergized case. Of the incident dust 70%  $\pm$  2% on average was ejected and landed on the funnel and 21%  $\pm$  2% was vaporized or ejected beyond the funnel. The above uncertainties are from the 0.1 mg readout precision of the balance and the standard deviation of the missing mass and derived ratios, added in quadrature. Fig. 3(b) shows the results for the chimney + roof configuration. Averaging over the 50 and 75  $\mu\text{m}$  grid results, 83% the incident dust was ejected when the grid was energized. The result for the 50  $\mu\text{m}$  trace/space grid

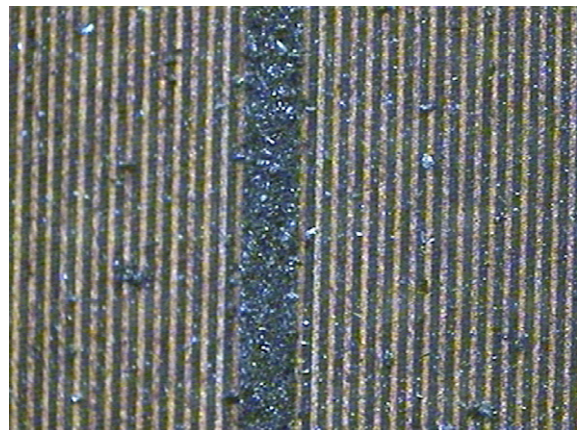


Fig. 2. Image of circuit grid with one trace open circuit. Incident dust particles are largely absent from the energized traces, in contrast to the high density of dust remaining along the open circuit trace. The trace width is 50  $\mu\text{m}$ .

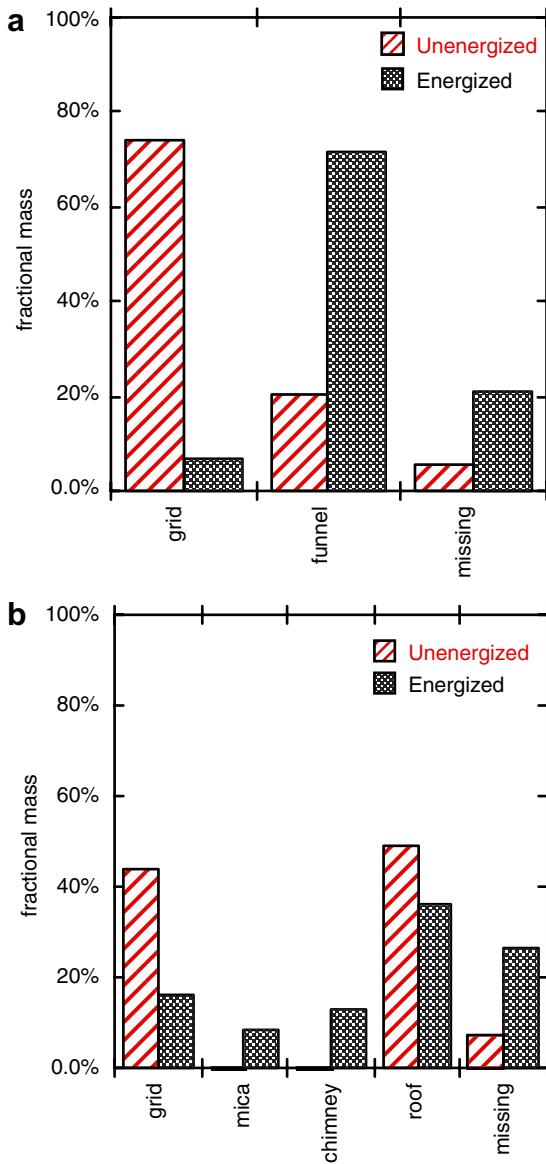


Fig. 3. Histograms showing the fraction of the mass lost from the dust container that accumulated on the various components under vacuum with an unenergized or energized grid. Plot (a) shows data obtained using the funnel and (b) obtained with the chimney and roof systems shown in Fig. 1. Up to 90% of the mass is vaporized or relocated when the grid is energized. 'Missing' mass is the difference between the total initial and final mass of dust on all components.

alone was 91%, similar to the funnel case. The mica mat and chimney showed significant mass gain in the energized case. Of the dust incident on the grid  $60\% \pm 8\%$  was ejected and landed on the chimney or mica and  $22\% \pm 10\%$  was vaporized or ejected beyond the roof.

The removal efficiency would be even higher without the single open trace on the circuit board used for the funnel trials and the first of the four chimney trials. The higher ejection fraction observed with the  $50\ \mu\text{m}$  grid for the chimney + roof configuration suggests that  $25\ \mu\text{m}$  grids would perform even better. On the third of the funnel trials about 1 mg of dust fell from the funnel onto the circuit board during the weighing process. During the first energized trial with the chimney and roof, particles were shaken down for 30 s as usual, however the counting electronics continue to show rapid counts for 45 s, indicating the particles were bouncing around inside the chimney for some time before being vaporized or sticking to the chimney or wiggling between mica mat and the flange. It turned out that mica was not a good choice for the insulator between the stainless chimney and grid as it trapped ejected dust particles and this sometimes lead to short circuits.

The experiment with the chimney was repeated with the same procedure except that the chamber was not evacuated and the results are shown in Fig. 4. The amount of dust used was reduced as it was easier to overload the grid in air, and this increased the measurement uncertainty. The dust incident on the energized grid was calculated from the mass lost by the dust container, less that which

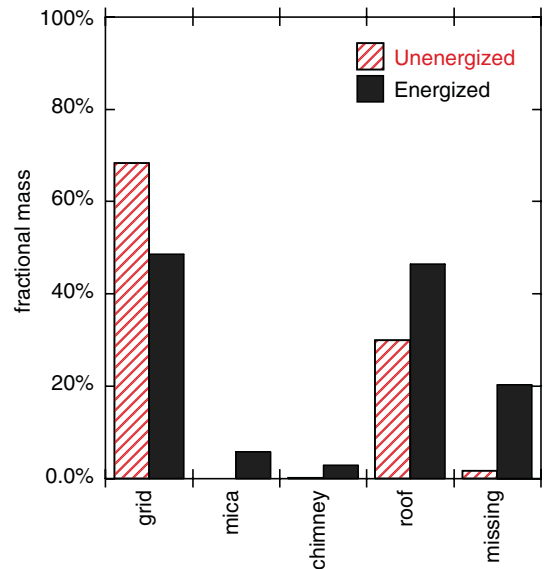


Fig. 4. Histogram showing the fraction of the mass lost from the dust container that accumulated on the various components under atmospheric pressure with an unenergized or energized grid. 'Missing' mass is the difference between the total initial and final mass of dust on all components.

landed on the roof, minus that lost to pumpout for the unenergized case. Of the incident dust  $51\% \pm 14\%$  remained on the energized grid,  $18\% \pm 10\%$  was relocated on the mica and chimney and  $31\% \pm 20\%$  was vaporized or ejected beyond the chimney and roof. The increase in fraction vaporized is believed to be due to oxidation in air.

#### 4. Dust detection in tokamaks

Dust has previously been collected from NSTX during a maintenance period and characterized [12]. Real-time measurements were attempted by installing two grids in NSTX on a vertical port 60 cm below the outer divertor at Bay C. A  $4.8 \text{ cm}^2$  glass slide positioned in between the grids was used to passively collect dust. A few counts were occasionally observed by the dust detection electronics [9] however these persisted when the grid was positioned vertically and covered with mica and it was concluded that these were due to electrical pickup. Dust levels were also measured by weighing the dust collected by the glass slide with a  $2 \mu\text{g}$  precision balance. A mass of  $34 \mu\text{g}$  of dust was accumulated over 1249 discharges of cumulative duration 702 s, or  $5.6 \text{ ng/cm}^2/\text{discharge}$ . This level is below the estimated sensitivity of  $36 \text{ ng/cm}^2/\text{count}$  of the grid detector and is consistent with the lack of dust signals. A large area detector is planned to increase the sensitivity and permit measurements on current tokamaks. We note that the ITER dust limit of 100 kg evenly distributed on the lower part of the machine amounts to  $\sim 60 \text{ mg/cm}^2$  so sensitivity will not be an issue for ITER.

In summary laboratory tests have showed that up to 90% of the amount of dust incident on the energized grid was ejected or vaporized. A mosaic of these devices based on nanoengineered traces on a low activation substrate such as  $\text{SiO}_2$  could be envis-

aged for remote inaccessible areas in a next-step tokamak. This mosaic would both detect conductive dust settling on surfaces in these areas and could ensure that these surfaces remained substantially dust free.

#### Acknowledgments

The authors thank T. Holoman, and T. Provost for technical assistance and A. Daruber for the use of a precision analytical balance. C. Parker acknowledges support from the 2005 National Undergraduate Fellowships in Plasma Physics and Fusion Energy Sciences. This work was funded by US DOE Contract Nos. DE-AC02-76CH0307.

#### References

- [1] G. Federici, C.H. Skinner, J.N. Brooks, J.P. Coad, C. Grisolia, A.A. Haasz, A. Hassanein, V. Philipps, C.S. Pitcher, J. Roth, W.R. Wampler, D.G. Whyte, Nucl. Fus. 41 (2001) 1967.
- [2] G. Federici, Phys. Scr. T124 (2006) 1.
- [3] C.H. Skinner, J.P. Coad, G. Federici, Phys. Scr. T111 (2004) 92.
- [4] C.H. Skinner, G. Federici, Phys. Scr. T124 (2006) 18.
- [5] J. Winter, Plasma Phys. Controll. Fusion 40 (1998) 1201.
- [6] M. Rubel, M. Cecconello, J.A. Malmberg, G. Sergienko, W. Biel, J.R. Drake, A. Hedqvist, A. Huber, V. Philipps, Nucl. Fusion 41 (2001) 1087.
- [7] Ph. Chappuis et al., J. Nucl. Mater 290&291 (2001) 245.
- [8] Radiological source terms, in: ITER Technical Basis, ITER EDA Documentation Series No. 24, IAEA, Vienna, 2002, p. 13 (Chapter 5.3).
- [9] A. Bader, C.H. Skinner, A.L. Roquemore, S. Langish, Rev. Sci. Instrum. 75 (2004) 370.
- [10] C.H. Skinner, A.L. Roquemore, A. Bader, W.R. Wampler, Rev. Sci. Instrum. 75 (2004) 4213.
- [11] C. Voinier, C.H. Skinner, A.L. Roquemore, J. Nucl. Mater 346 (2005) 266.
- [12] J.P. Sharpe, P.W. Humrickhouse, C.H. Skinner, the NSTX team, T. Tanabe, K. Masaki, N. Miya, the JT-60U Team, A. Sagara, J. Nucl. Mater. 337–339 (2005) 1000.